

SUPPLEMENTARY MATERIAL

Particle size effect on the microstructure and the aging process of flash-sintered barium titanate from micro and nanopowders

Samuel López-Blanco,^{1,*} Xavier Vendrell,² Lourdes Mestres,² Diego A. Ochoa¹, and Jose E. García¹

¹ Department of Physics, Universitat Politècnica de Catalunya – BarcelonaTech, 08034 Barcelona, Spain.

² Department of Inorganic and Organic Chemistry, Universitat de Barcelona, 08028 Barcelona, Spain.

* Corresponding author: samuel.lopez.blanco@upc.edu (S. Lopez-Blanco).

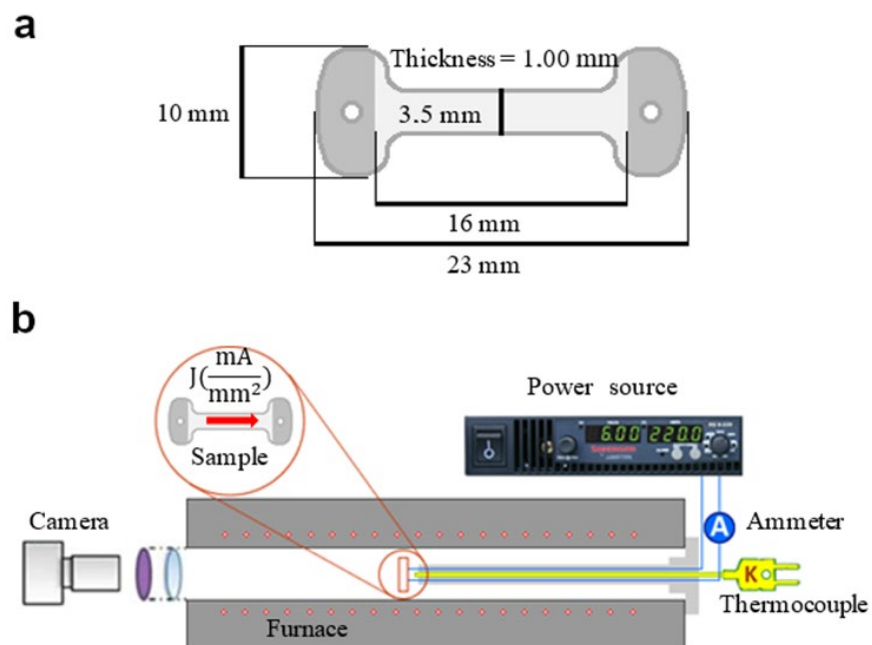


Fig. S1. (a) Green sample dimensions after uniaxial pressing and (b) typical flash sintering experimental setup scheme. Dark grey regions in the sample represent platinum painted electrodes.

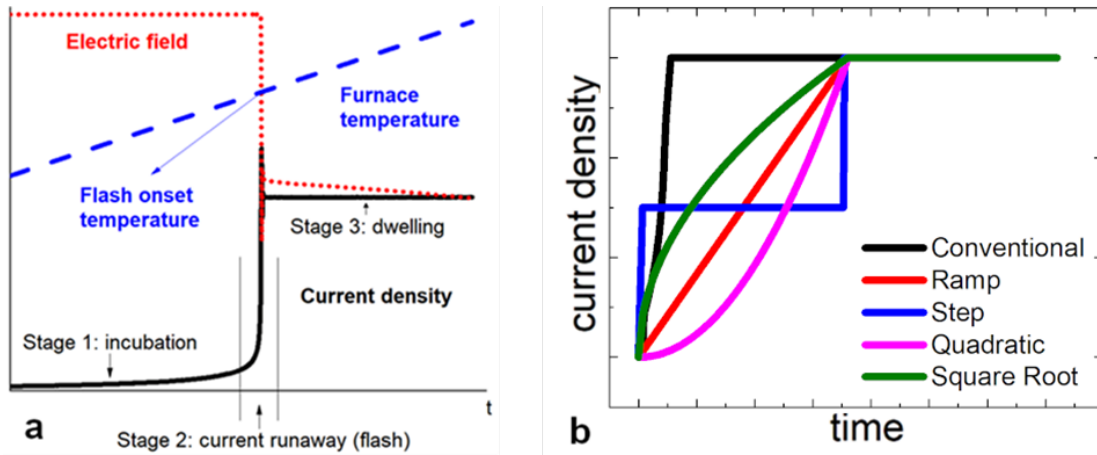


Fig. S2. (a) Conventional flash sintering scheme and (b) current controlled flash sintering (CCFS) profiles. CCFS current profiles are selected so that every experiment reaches maximum current density in the same time (except the conventional flash experiment, in which the sample undergoes current runaway almost instantly). Samples are then left to dwell for a set period.

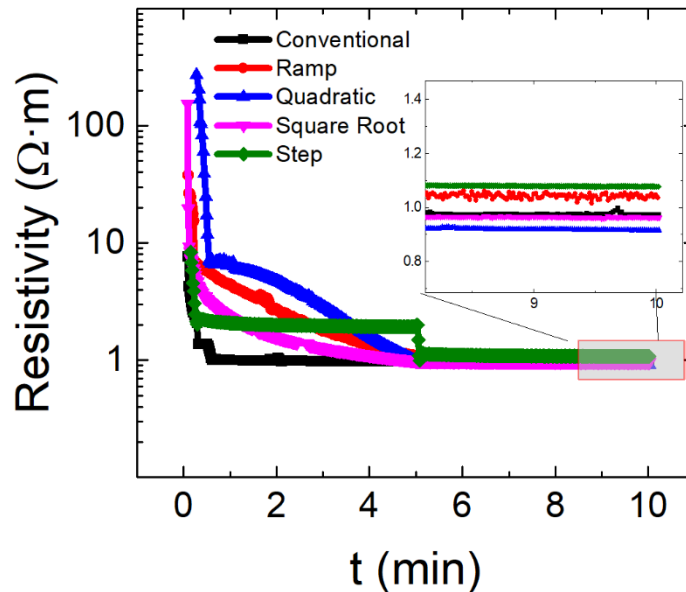


Fig. S3. Resistivity evolution of samples sintered with different electric current profiles, at 950 °C and 15 mA/mm². Instantaneous resistivity values during the current control regime depend on the selected current profile. During the dwell time, when the same electrical conditions are applied, all samples show similar values of resistivity.

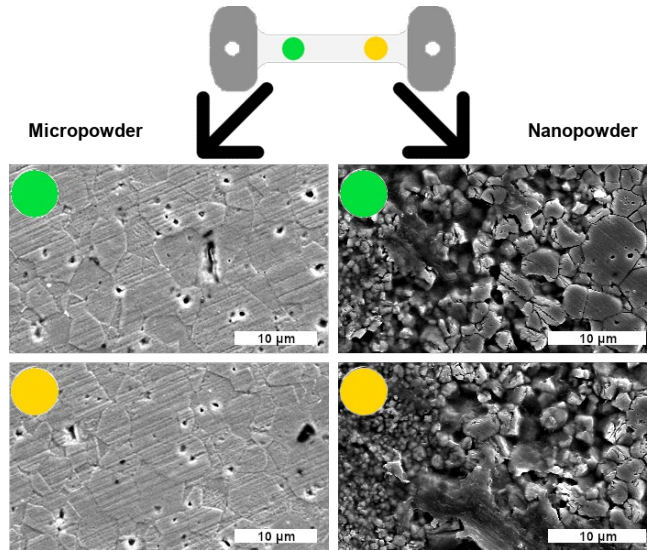


Fig. S4. Schematic representation of the sintered specimen (“dog bone” shaped) and the final sample after cutting, removing the electrodes. Below, SEM micrographs of two extreme zones of a final sample are shown for both micropowder and nanopowder cases. Electrical conditions are 150 V/cm and 15 mA/mm².

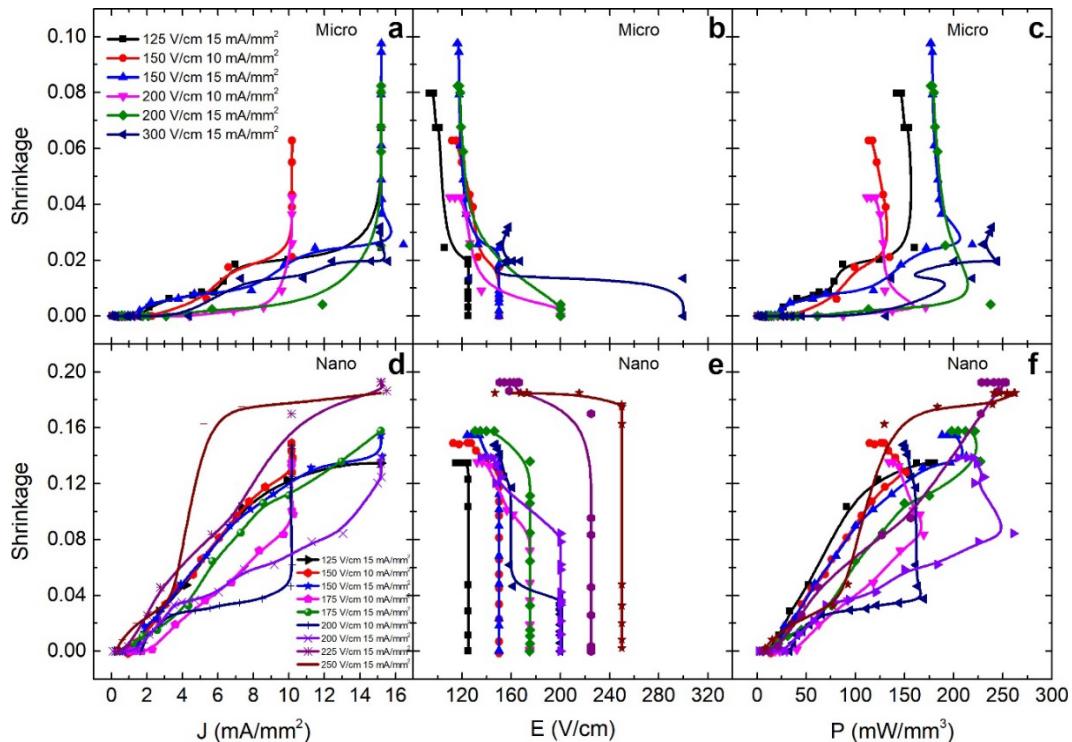


Fig. S5. Shrinkage profile of samples obtained from nanopowder and micropowder, sintered under different electrical conditions. Electric current, electric field, and total electric power are correlated with optically measured shrinkage of the samples along the electric field axis. Differentiated shrinkage behaviors are observed, which corresponds to different powders and electrical conditions.

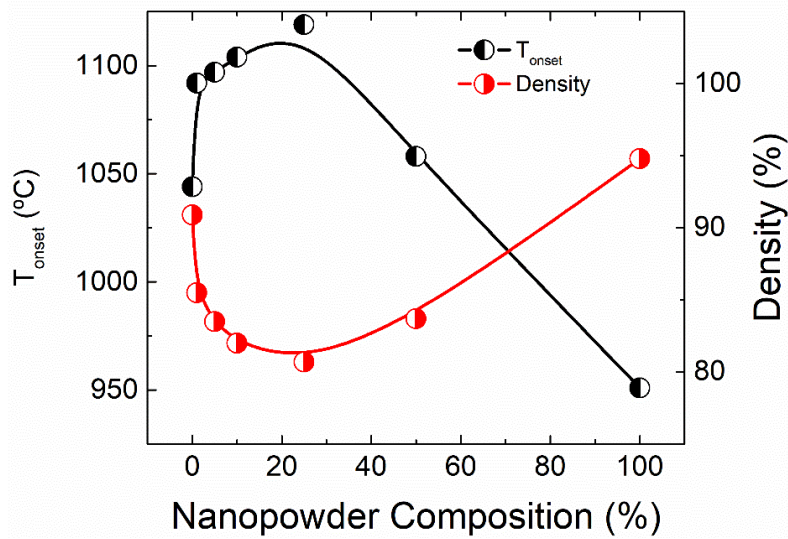


Fig. S6. Density and flash onset temperature of nano-micro mixture powder samples sintered at 150 V/cm and 10 mA/mm². Dwell has been maintained at 10 minutes for all cases. Employed compositions are 0%, 1%, 5%, 10%, 25%, and 50% nanopowder content.

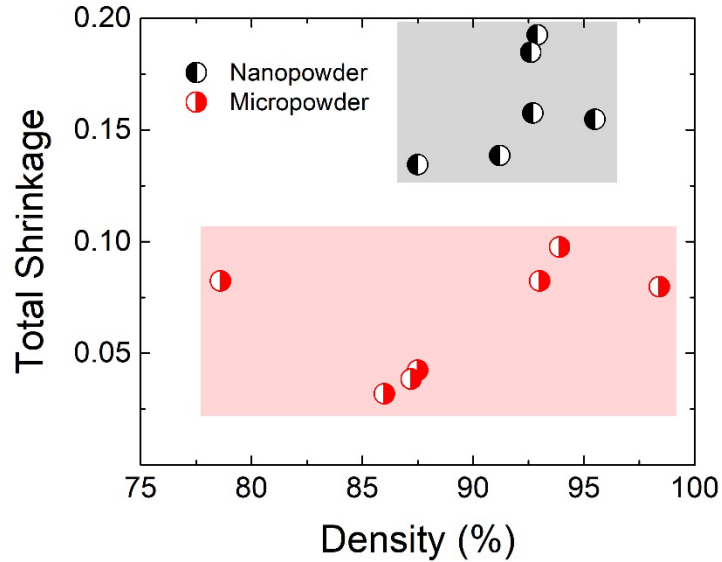


Fig. S7. Shrinkage relation to density for conventional flash-sintered samples under different electrical conditions. No correlation is found between both magnitudes, thereby concluding that density measured with the Archimedes method is preferred to the optical shrinkage, which will be used only as a qualitative analysis tool.

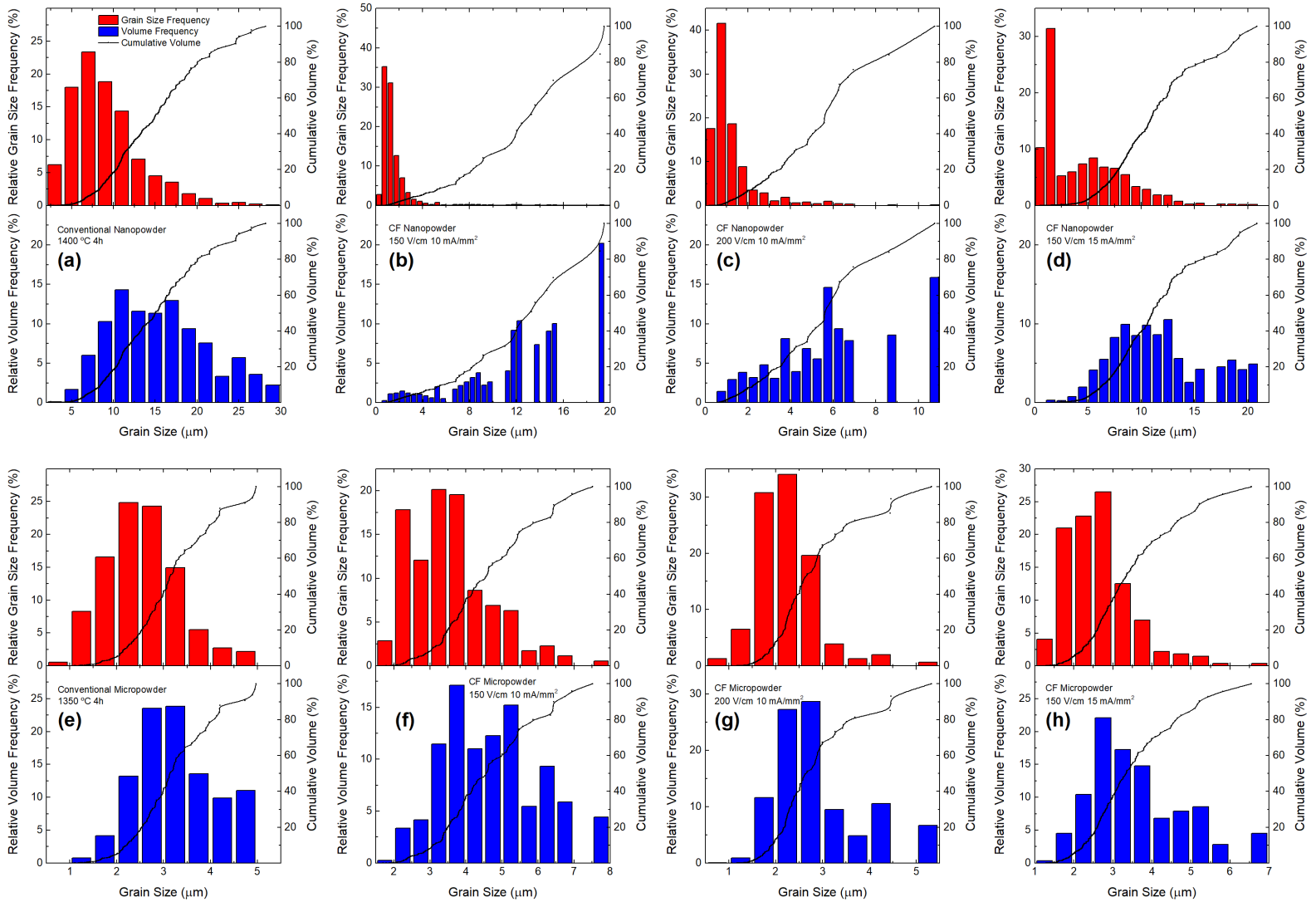


Fig. S8. Grain size distribution, grain volume distribution and cumulative volume of samples sintered under different conventional flash sintering conditions obtained from (b-d) nanopowders or (f-h) micropowder. Results for conventional sintered samples (a,e) are also plotted. Higher electric fields tend to hinder the formation of huge abnormal grains for the case of samples obtained from nanopowder (c), and increasing electric current forms a bimodal distribution (d). For the case of samples obtained from micropowder no abnormal distribution is recorded regardless of the electrical sintering conditions.

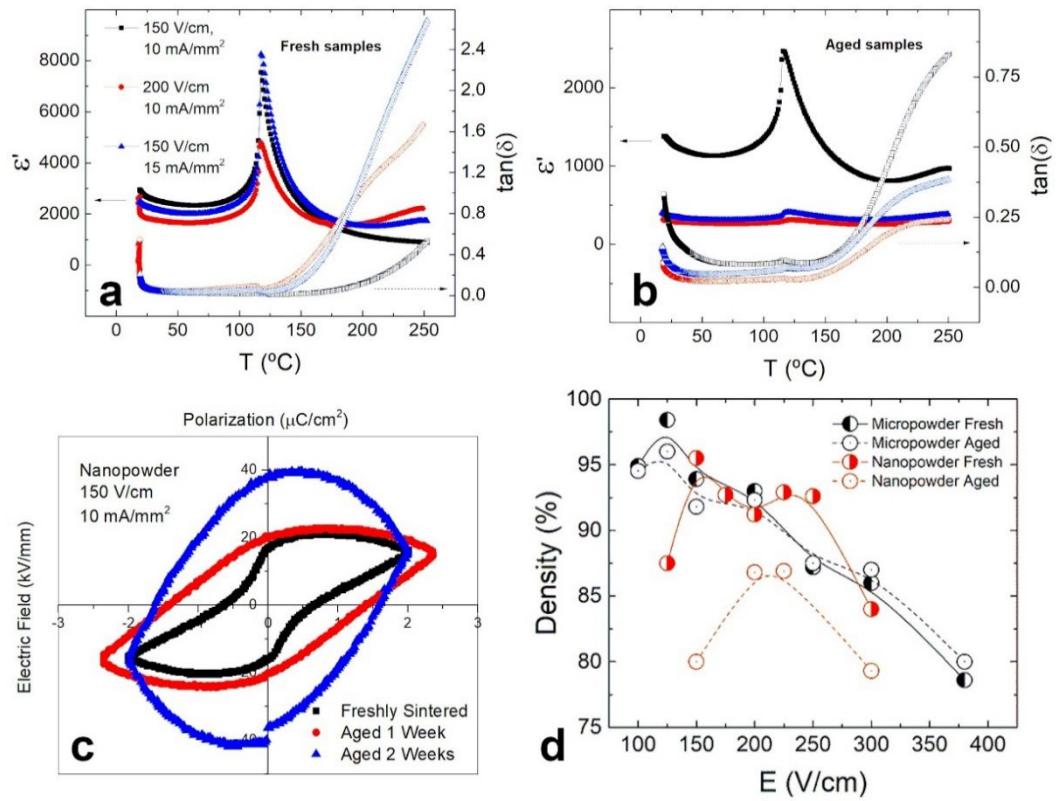


Fig. S9. Dielectric response of BTO samples sintered from nanopowder under different electrical conditions measured (a) a day after sintering and (b) two weeks after sintering. Real part of the dielectric permittivity is represented with filled points while the loss tangent is represented using hollow points. Dwell times have been maintained at 10 min for all cases. Both real and imaginary parts of the dielectric permittivity display a sharp decrease with time, manifesting strong evolution of the functional properties. (c) Hysteresis loop of a flash-sintered sample obtained from nanopowder measured at different times. (d) Time evolution of density of samples sintered using different starting powders after a year of storage in ambient atmosphere.

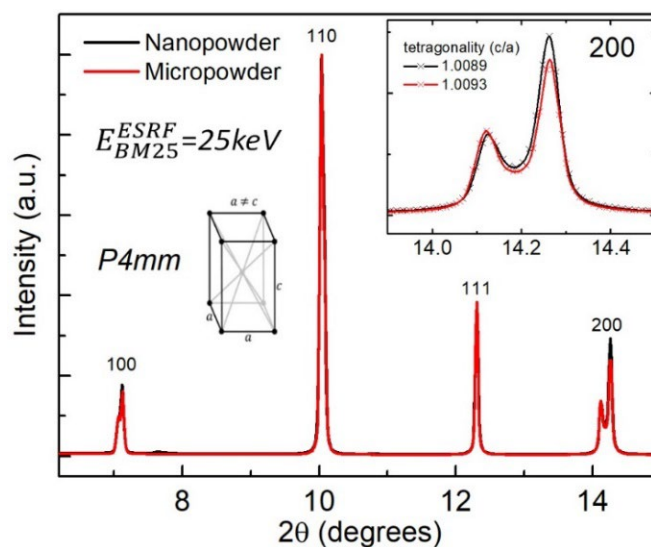


Fig. S10. X-ray diffraction (XRD) patterns of conventional flash-sintered samples at 150 V/cm and 15 mA/mm² using different starting powders. Diffraction patterns were measured using high-energy synchrotron radiation at the beamline BM25 of the European Synchrotron Radiation Facility (ESRF). The samples were placed into a six-circle diffractometer (SixC) and irradiated in transmission mode using an X-ray beam of 25 keV and 0.1 mm x 0.1 mm. A 2D CCD detector was used to collect the XRD data.

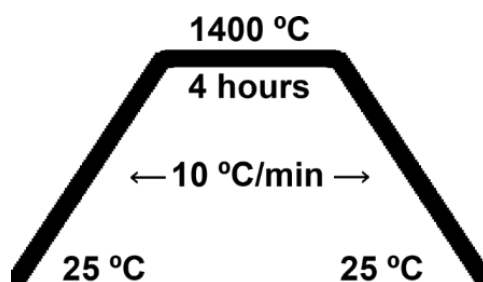


Fig. S11. Schematic representation of the conventional sintering process. Sample is heated and cooled using a constant rate ramp of 10 °C/min. Upon reaching 1400 °C, the sample is dwelling for 4 hours.

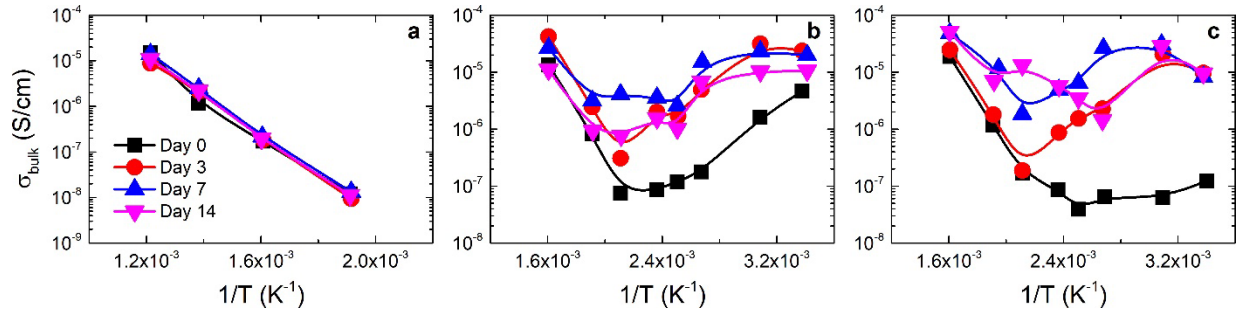


Fig. S12. Time evolution of conductivity for: (a) flash-sintered BTO from micropowder at 150 V/cm and 15 mA/mm², (b) flash-sintered BTO from nanopowder at 150 V/cm and 10 mA/mm², and (c) flash-sintered BTO from nanopowder at 150 V/cm and 15 mA/mm². While the sample flash-sintered from micropowder stays constant with time, both flash-sintered samples from nanopowders undergo a complex evolution that heavily change their conductivity for all temperature ranges.

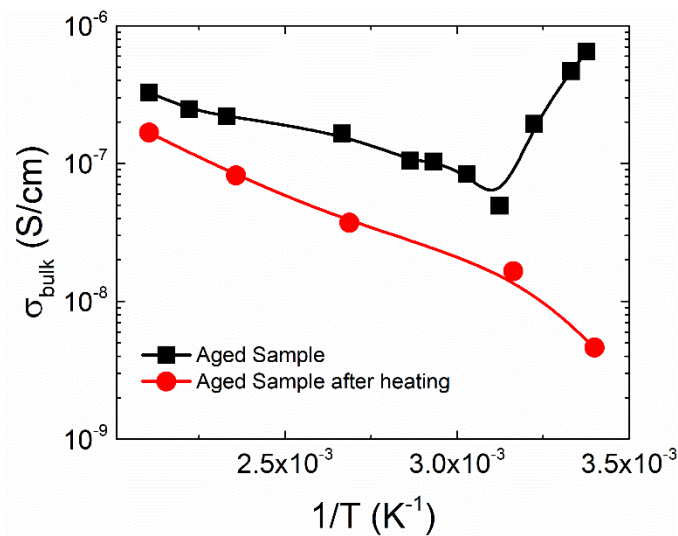


Fig. S13. Conductivity behavior for an aged sample before and after heating above 200 °C. Notice that the low temperature electronic-like behavior disappears after the heating the samples at 250 °C, indicating the presence of possible defect recombination.

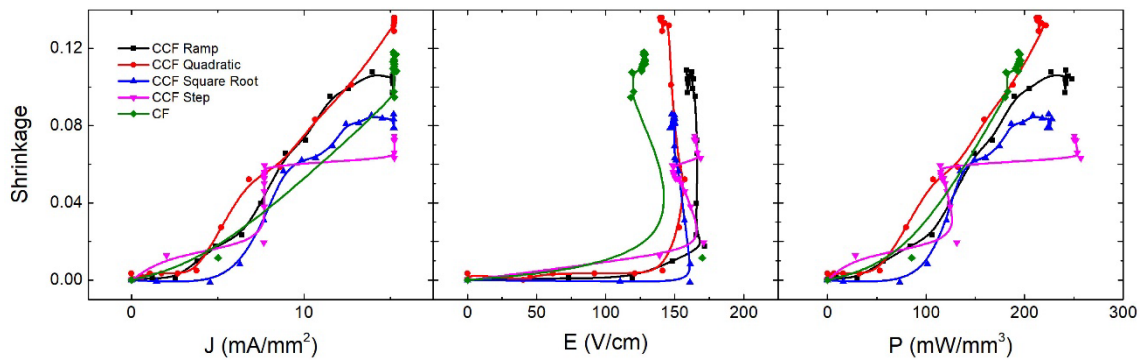


Fig. S14. Shrinkage profile of samples sintered from nanopowder under different CCFS conditions. Furnace temperature is held at 950 °C and dwell time is 5 min for all cases. Electric current, electric field and total electric power are correlated with optically measured shrinkage of the samples along the electric field axis.

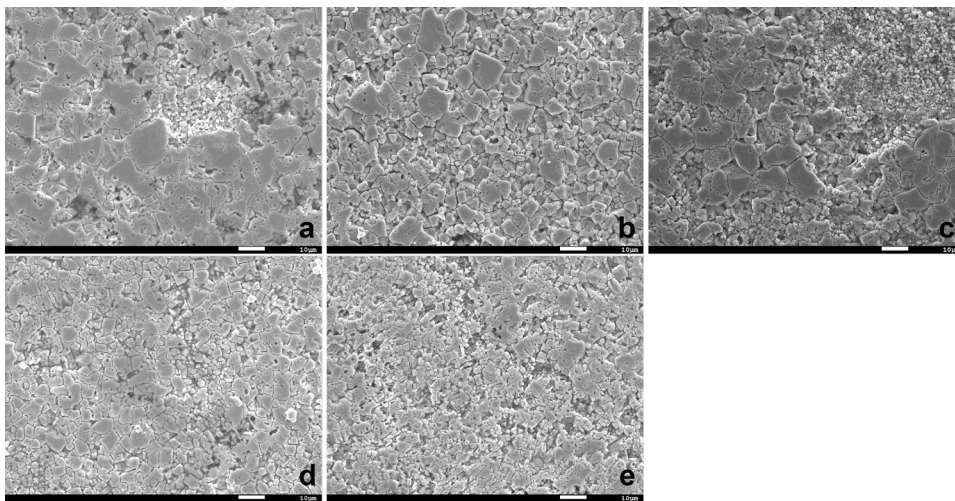


Fig. S15. Microstructure of CCFS samples sintered at 950 °C and 5 min of dwell time using different current profiles: (a) ramp, (b) step, (c) quadratic, and (d) square root. (e) Microstructure of conventional flash-sintered sample (i.e., without a current profile) is also shown from comparison.

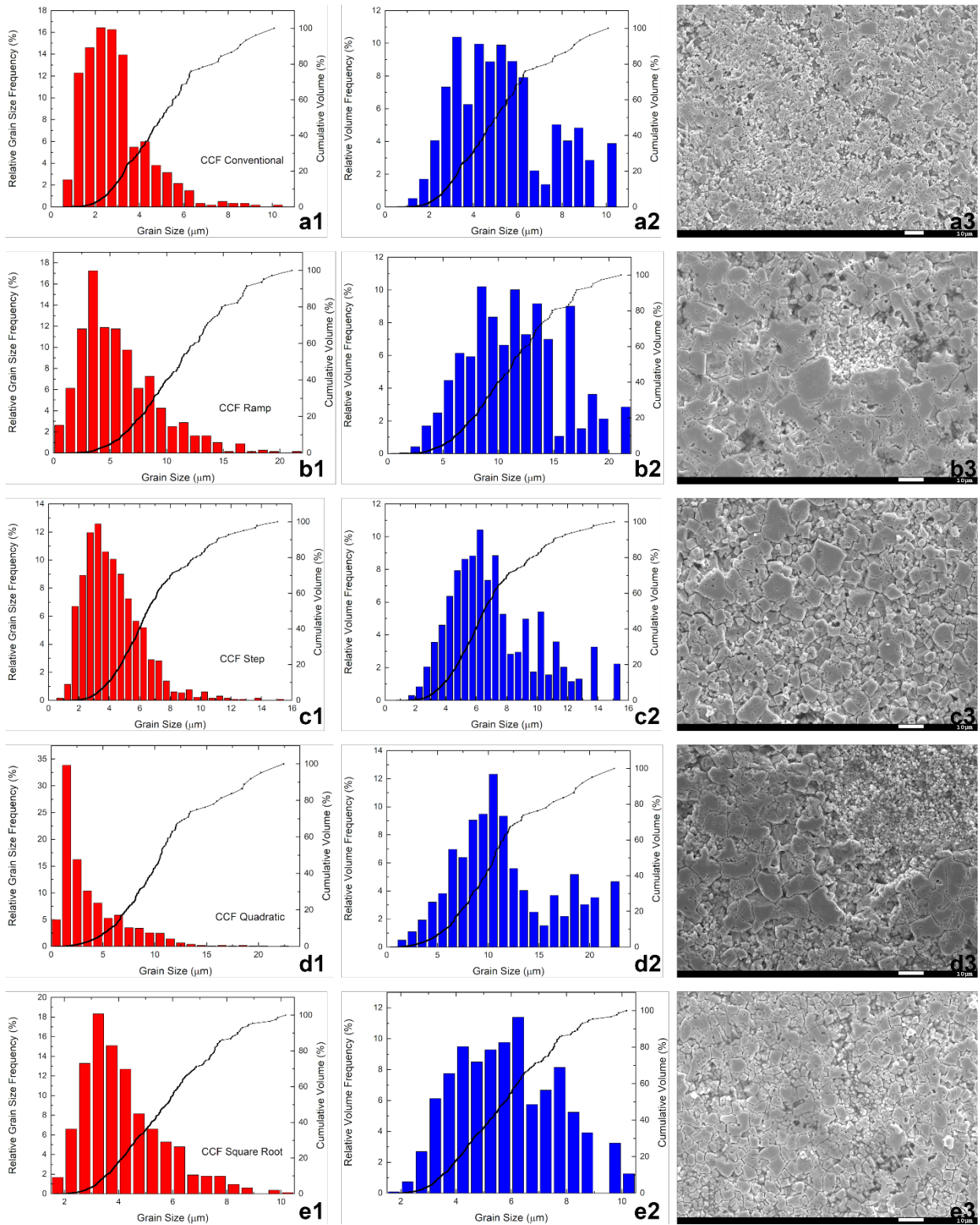


Fig. S16. Grain size distribution, grain volume distribution, cumulative volume and SEM micrograph of samples sintered under different CCFS conditions.

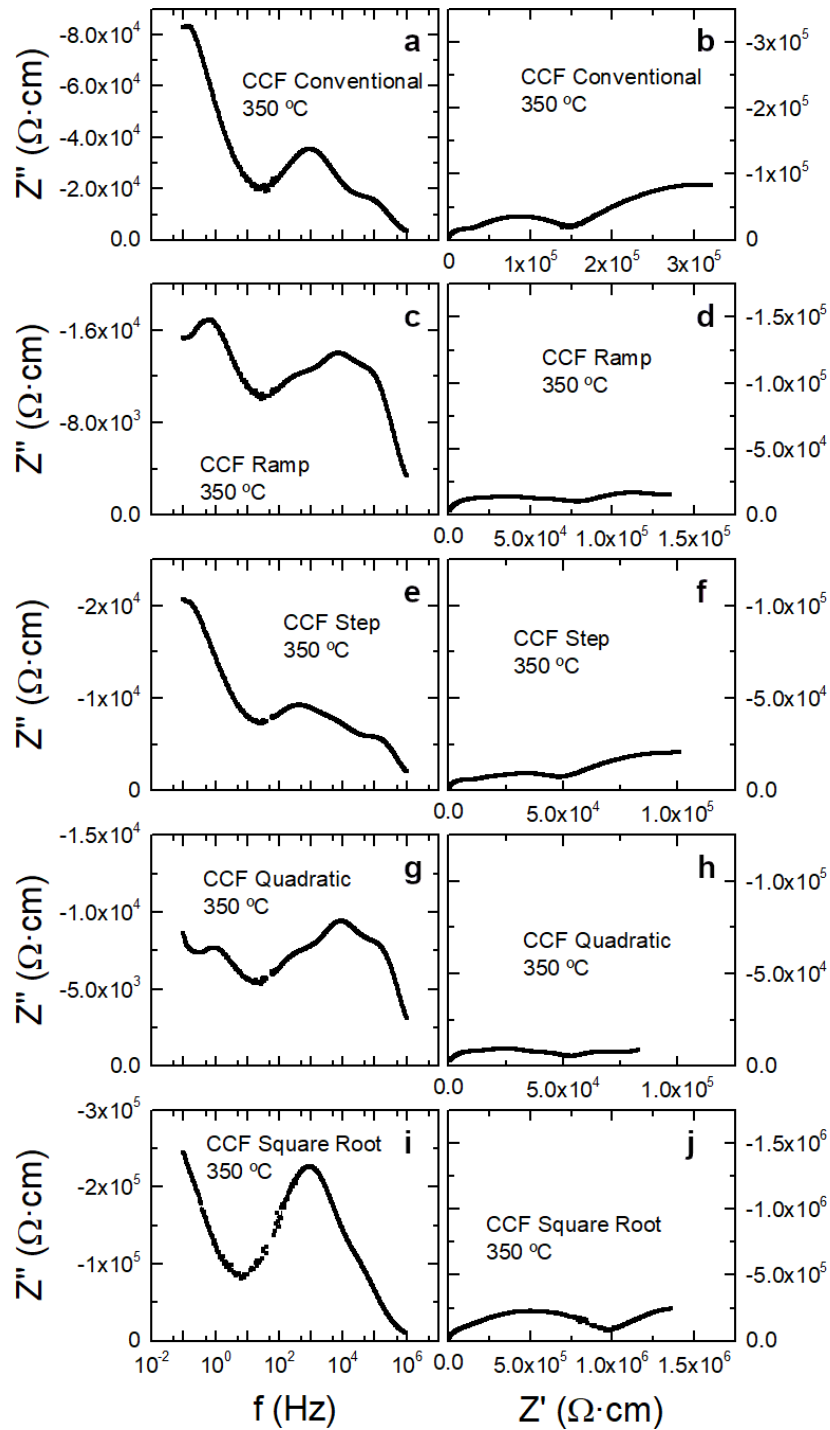


Fig. S17. (a, c, e, g, i) Frequency dependence of the imaginary part of the impedance and (b, d, f, h, j) Nyquist plots for CCF samples under different current profiles. Note that CCF samples using ramp (c, d), step (e, f) or quadratic (g, h) current profiles exhibit a fourth contribution to the impedance, which qualitatively is evidenced by the existence of a fourth semicircle in the Nyquist plots and a fourth local maximum in the Z'' vs frequency curves.

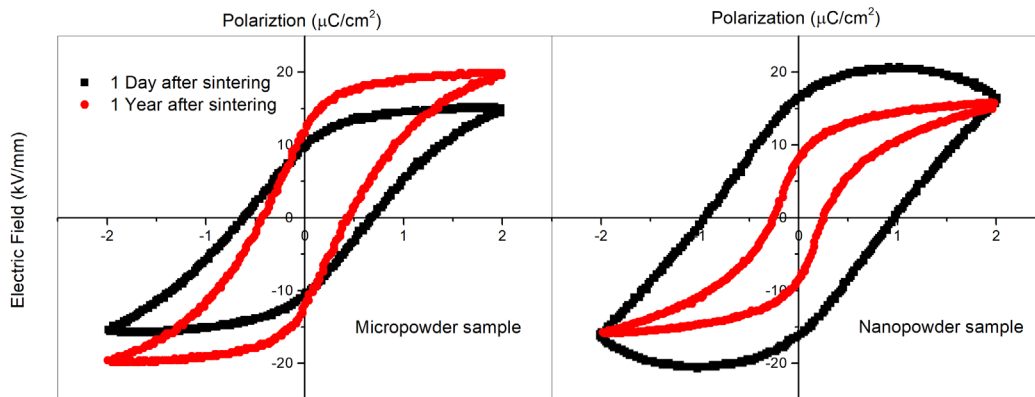


Fig. S18. Hysteresis loops of conventional-sintered samples from both micro and nanopowders. The conduction related to the formation of oxygen vacancies during sintering disappears after a long exposure to ambient atmosphere.

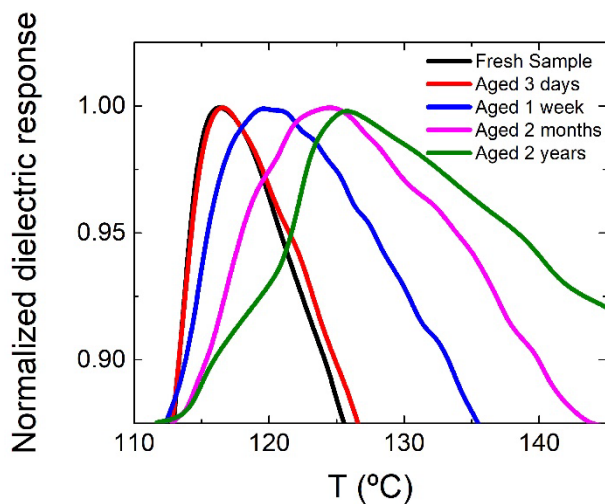


Fig. S19. Maximum of the real permittivity corresponding with the ferroelectric to paraelectric phase transition of a flash-sintered sample from nanopowder at 150 V/cm and 10 mA/mm². The temperature at which the maximum occurs evolves with time.

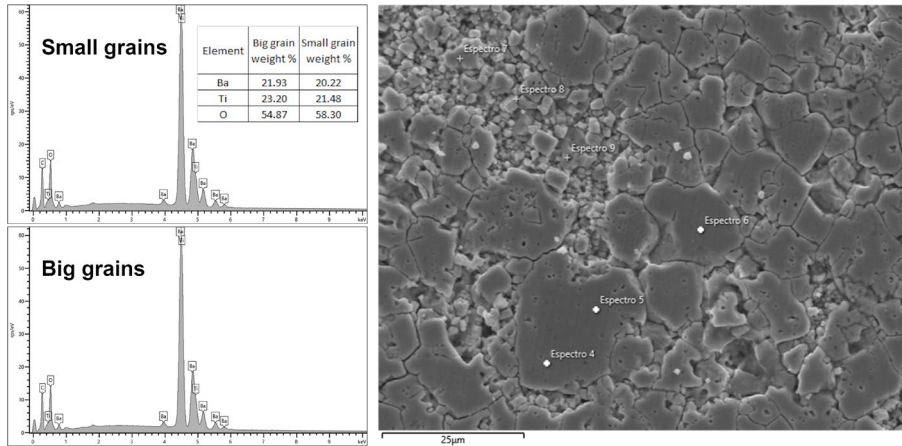


Fig. S20. EDS spectra of a flash-sintered sample using quadratic current profile. Data are taken in grains of different sizes. Abnormally grown grains exhibit less concentration of oxygen, which is attributed to lattice reduction during flash sintering.

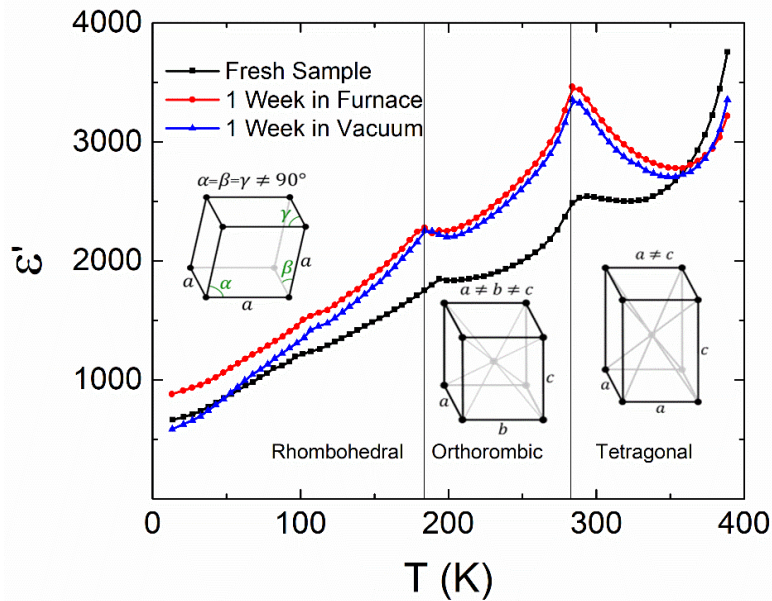


Fig. S21. Low temperature evolution of the dielectric response of a sample after different treatments. After heat treatment a clear shift of the tetragonal-orthorhombic and orthorhombic-rhombohedral transitions towards lower temperature takes place. Intrinsic dielectric response also increases, indicating a change in the unit cell structure. After treating the same sample in vacuum, the intrinsic dielectric response lowers again.